Review of European Studies; Vol. 8, No. 1; 2016
ISSN 1918-7173 E-ISSN 1918-7181
Published by Canadian Center of Science and Education

Evaluation of the Reduction of Tsunami Damages Based on Local Wisdom Contermeasures in Indonesia

Fadly Usman[1], Agus Dwi Wicaksono[1] & Eko Setiawan[2]

[1] Department of Urban and Regional Planning, Brawijaya University, Indonesia

[2] Faculty of Computer Science, Brawijaya University, Indonesia

Correspondence: Fadly Usman, Department of Urban and Regional Planning, Brawijaya University, MT Haryono 167, Malang, 65145, Indonesia. Tel: 62-821-3130-5081. E-mail: fadlypwk@ub.ac.id

Received: January 8, 2016 Accepted: Januray 27, 2016 Online Published: February 13, 2016

doi:10.5539/res.v8n1p157 URL: http://dx.doi.org/10.5539/res.v8n1p157

Abstract

Local wisdoms such as a traditional ethics, land-use system and others had sometimes mitigated tsunami damages in Indonesia. The effective use of those local wisdoms is strongly desired especially in developing countries, because it is quite difficult for those countries to allocate enough budgets for constructing hard type of countermeasures against tsunami. Among local wisdoms against tsunami hazard, this study evaluates the efficiency of a hollow topography which can be seen on the beach along Lampon village in Indonesia. Artificial hollows are arrayed on the beach as one of the local wisdoms in Lampon village to reduce the intensity of inundated tsunami flow. The numerical simulation of tsunami inundation is conducted to evaluate the efficiency of this hollow topography. Furthermore, this study evaluates the efficiency of some contrivances, such a combination of vegetation area and a multiple-use of hollow and embankment topography, in order to enhance the performance of countermeasure based on the local wisdom.

Keywords: Tsunami, local wisdom, numerical simulation, local wisdom countermeasure

1. Introduction

Local wisdoms such as a tradition, land-use system, etc. had sometimes mitigated tsunami damages in Indonesia. For example, a tradition of early evacuation had been handed down in Simeulue Island since their catastrophic tsunami experience in 1907, and the tsunami in 2004 killed only 6 peoples in this island. The effective use of local wisdoms is strongly desired especially in developing countries, because local governments cannot allocate enough budgets for constructing hard type countermeasures against tsunami.

Among those local wisdoms against tsunami hazard, this study evaluates the efficiency of a hollow topography which can be seen on the beach along Lampon village in Indonesia. Hollow topography means a low ground that is locally dug by residential people in order to reduce the intensity of tsunami flow as one of the countermeasures based on the local wisdom.

Lampon village in Banyuwangi on Java Island had experienced an earthquake with magnitude 7.6 in 1994. A sizeable tsunami hit this coast 50 minutes after the main shock. According to the research results of Tsuji et al. (1995), the tsunami height at a point in Lampon village was measured as 5.4m. On the other hand, 9.1m tsunami height was also measured at a point on the seaside 1km east of the village. Between these two points, there is a vegetation area and an artificially hollowed area. At this earthquake, those topographic features might have reduced the tsunami energy in Lampon village.

An aerial photo in Figure1 introduces a typical coastal area in Lampon village. A vegetation area and a hollow topography can be seen in this photo. There are some artificial hollows on this beach, and their averaged size is about 100 m in length, 20 m in width and 2 m in depth. This study evaluates the efficiency of the hollow topography in reducing tsunami inundation depth and velocity. Two-dimensional numerical analysis is conducted in this study to investigate the inundation flow over the hollow topography. Furthermore, this study evaluates the efficiency of some contrivances, such a combination of vegetation area, a multiple-use of hollow and embankment topography in order to enhance the performance of countermeasure based on the local wisdom.

2. Method

2.1 Numerical Simulation Method

This study employs Cadmas-Surf/2D to conduct a numerical simulation (CADMAS-Surf user manual, 2001). The governing equations consisted of a continuity equation, Navier-Stokes equation in x and z direction and an advection equation for tracing the temporal water surface elevation. The last equation includes the function, $F(x,z,t)$, which means the ratio of water volume in each numerical cell.

$$\frac{\partial \gamma_x u}{\partial x} + \frac{\partial \gamma_z w}{\partial z} = S_p \tag{1}$$

$$\lambda_v \frac{\partial u}{\partial t} + \frac{\partial \lambda_x uu}{\partial x} + \frac{\partial \lambda_z wu}{\partial z} = -\frac{\gamma_v}{\rho}\frac{\partial p}{\partial x} + \frac{\partial}{\partial x}\left\{\gamma_x v_e \left(2\frac{\partial u}{\partial x}\right)\right\} + \frac{\partial}{\partial z}\left\{\gamma_z v_e \left(\frac{\partial u}{\partial z} + \frac{\partial w}{\partial x}\right)\right\} - D_x u + S_u - R_x \tag{2}$$

$$\lambda_v \frac{\partial w}{\partial t} + \frac{\partial \lambda_x uw}{\partial x} + \frac{\partial \lambda_z ww}{\partial z} = -\frac{\gamma_v}{\rho}\frac{\partial p}{\partial z} + \frac{\partial}{\partial z}\left\{\gamma_z v_e \left(2\frac{\partial w}{\partial z}\right)\right\} + \frac{\partial}{\partial x}\left\{\gamma_x v_e \left(\frac{\partial w}{\partial x} + \frac{\partial u}{\partial z}\right)\right\} - D_z w + S_w - R_z - \gamma_v g \tag{3}$$

$$\gamma_v \frac{\partial F}{\partial t} + \frac{\partial \gamma_x uF}{\partial x} + \frac{\partial \gamma_z wF}{\partial z} = S_F \tag{4}$$

In above equations, t means the time, x and z means the horizontal and vertical coordinate. Also, p means the pressure, u and w means the horizontal and vertical velocity components, respectively. ρ is the density of fluid, v is the summation of molecular kinematic viscosity and eddy kinematic viscosity, g is the gravity acceleration. v_γ is the volume porosity, γ_x and γ_z are the aerial of porosity components, S_F, S_u, and S_w are wave generation source, D_x and D_z are the coefficient for sponge layer, and R_x and R_z are the resistant components due to porosity in x and z axis.

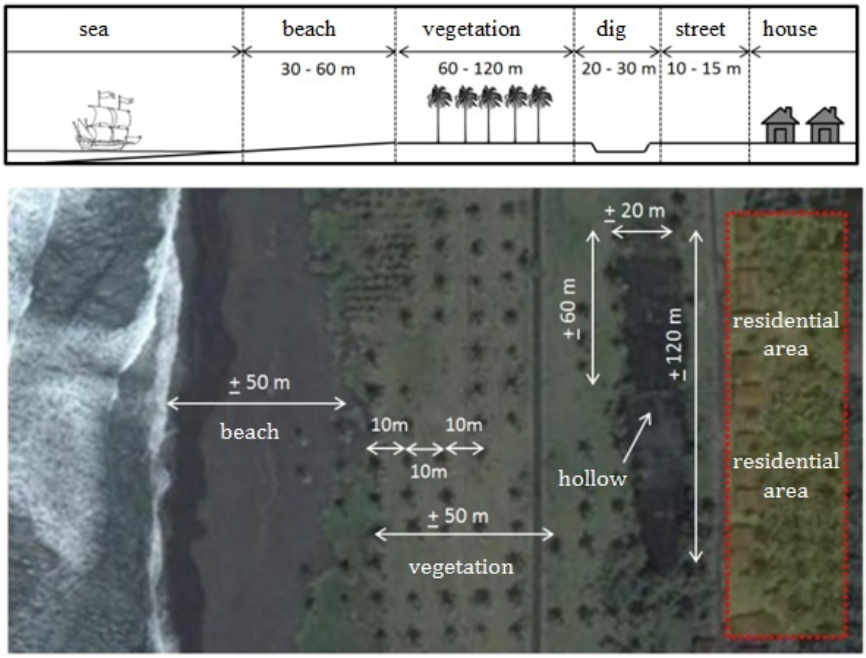

Figure 1. Typical beach configuration in Lampon Village

2.2 Numerical Wave Flume

Figure1 shows the longitudinal profile and the plane view of a beach in Lampon village. A sandy beach with 30m to 60m in width can be seen along this village. There is a vegetation area after sandy beach. The width of vegetation area is about 60m to 120m. The hollow topography is located between vegetation area and residential one as seen in Figure 1. The hollow topography has about 120m in length, 20m in width and 2m in depth.

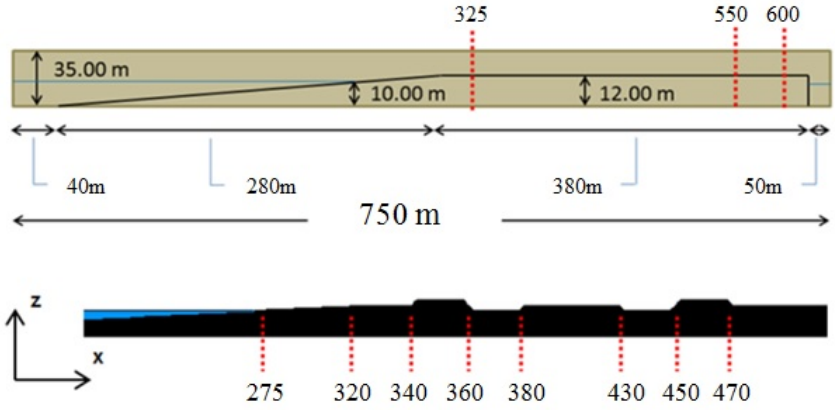

Figure 2. Schematics of numerical wave flume

According to the configuration of coastal topography on Lampon village, this study set the numerical wave flume as shown in Figure 2. The flume has 750 m in length and 35 m in height. The offshore wave depth is maintained as 10m as shown in the upper figure of Figure 2. A uniform sea bottom slope with 1/28 is set in the flume, and hollow topography is also set on a flat section. The lower figure in Figure 2 shows the location of hollows and embankment. This figure is Case-16, which is explained in letter section. The numerical grid in x and z direction is set as $\Delta x = 0.25$ m and $\Delta z = 0.25$ m, respectively.

2.3 Configuration of Numerical Simulation

This study considers embankment in addition to the hollow topography. Embankment could be formed with utilizing the dug materials obtained from hollow excavation. In numerical simulation, it is assumed that the topography in numerical flume is impermeable, and the topography keeps its original form even under the wave actions. Table 1 shows the list of numerical experiments conducted in this study. Sixteen cases in Table 1 consist of three groups, which are from Case-1 to Case-5, from Case-6 to Case-11 and from Case-12 to Case-16.

Case-1 has a simple slope without any special topography. Case-2 has a hollow topography. The hollow topography has a rectangular shape with 20m in length and 2m in depth. Case-3 is the single combination of hollow and embankment topography, where the hollow topography is set on the seaside of the embankment. The embankment has a rectangular shape with 20m in length and 2m in height. Case-4 is also the combination of embankment and hollow topography, where the embankment is set on the seaside of the hollow. This group includes the case of single embankment in Case-5, which is similar to the dike construction with 5m in length and 2m in height, it is set 320m from the beginning of the numerical flume.

Numerical experiments from Case-6 to Case-11 investigate the case of hollow and embankment topography with vegetation area. For example, Case-6 consists of an embankment, a hollow topography and a vegetation area, where each section is arrayed from the seaside to the landward. In this group, the vegetation area has 100m in width, and its porosity is set as 0.97 in numerical simulation according to the experimental studies by Harada (2002) and Suzuki (2010). The dimensions of hollow and embankment topography are the same as the first group.

Numerical experiments from Case-12 to Case-16 investigate the efficiency of the multiple-use of hollow and embankment topography in reducing tsunami flow. For example, Case-13 consists of four section, where hollow, embankment, hollow and embankment topography are arrayed from the seaside to the landward. The size of the hollow and embankment topography in this group is the same as the first group.

Table 1. List of numerical experiments in this study

CASE	Configuration of topography
1	Simple slope
2	Hollow
3	Hollow + embankment
4	Embankment + hollow
5	Seawall
6	Embankment + hollow + vegetation
7	Hollow + embankment + vegetation
8	Hollow + vegetation
9	Vegetation + hollow
10	Vegetation + hollow + embankment
11	Vegetation + embankment + hollow
12	Hollow + hollow
13	Hollow + embankment + hollow + embankment
14	Embankment + hollow + embankment + hollow
15	Hollow + embankment + embankment + hollow
16	Embankment + hollow + hollow + embankment

According to the averaged tsunami height observed in Lampon village, this study generates a bore type tsunami with 6m in height. CADMAS-Surf/2D requires the time history of water surface elevation and fluid velocity on an input boundary to generate waves with arbitrary profile. This study assumes the bore profile on the offshore region at first, and the velocity profile related to this bore profile is obtained by utilizing the following equation (Fukui; 1962 in Wijatmiko; 2010).

$$U = \frac{C\zeta}{H} = \zeta \sqrt{\frac{g(H+h)}{2H(H-\eta\zeta)}} \tag{5}$$

In this equation, U means the depth averaged velocity and g means the gravity acceleration. $H=h+\zeta$ means the total depth from datum and ζ also means the temporal bore height. η is a coefficient obtained from the ratio between the initial water depth on a propagation area the total depth of the propagating bore, and it is set as 1.03 in this study.

3. Results and Discussion

In this study, both water surface elevation and flow velocity are measured at three locations, 325m, 550m and 600m from the input boundary, as the reference points in order to evaluate the reduction effect of tsunami inundated flow on the inundation section as shown in Figure 2.

3.1 Numerical Simulation from Case-1 to Case-5

Figure 3 shows the snapshot of tsunami inundation in Case-2, Case-3 and Case-4. In Case-2, the small reflection of the inundated flow can be observed on the landward slope of the hollow topography when the flow over this hollow. This flow reflection becomes larger in Case-3 because the embankment behind the hollow increases the crest level on the landward slope.

On the other hand, the flow reflection at two sections can be observed in Case-4. One is on the landward slope of the hollow and the other is on the seaside slope of the embankment. Strong flow reflection observed in Case-3 and Case-4 reduces the inundated flow, and its depth and velocity becomes smaller in comparison with the simple hollow topography in Case-2.

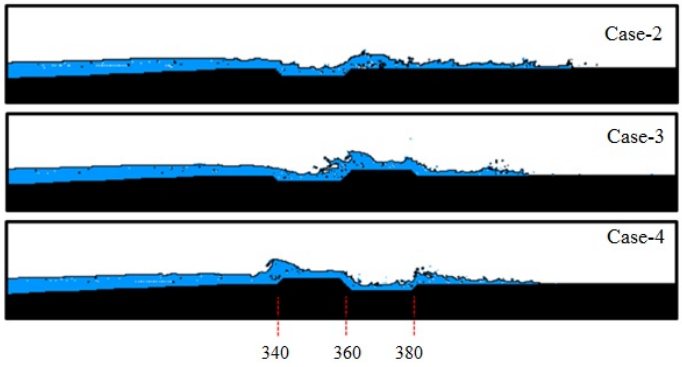

Figure 3. Snapshot of tsunami inundation at t=35 sec (Case-2 to Case-4)

Figure 4 shows the water surface profiles and velocity ones at 600m location from the input boundary. It is clear that the inundated flow depth and velocity are reduced in Case-3 and Case-4 in comparison with Case-2 and Case-5, though the Case-2 and Case-5 slightly reduce the flow depth and velocity in comparison with Case-1.

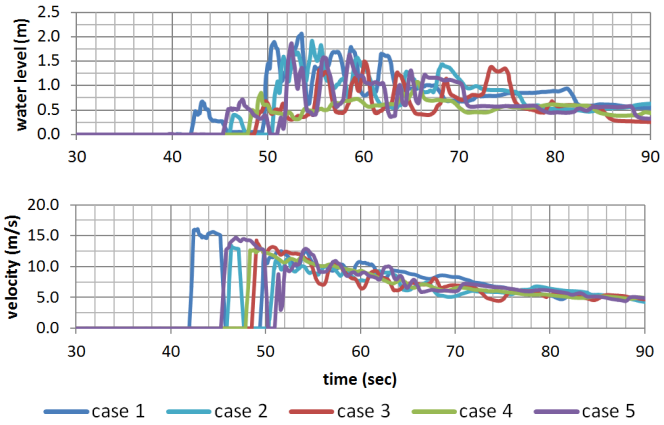

Figure 4. Profiles of inundated flow depth and velocity at 600m location (From Case-1 to Case-5)

Table 2 shows the maximum values of flow depth and velocity obtained from the profiles in Figure 4. Case-4 has the highest efficiency in reducing inundated flow depth and velocity in this group, and this advantage comes from the flow reflection at two sections as shown in Figure 3. Case-2 and Case -3 are also superior to the simple slope condition in Case-1, and Case-2 is inferior to Case-3.

Table 2. Maximum inundated flow depth and velocity at 325m, 550m and 600m locations (Case-1 to Case-5)

CASE	Water height			velocity		
	325 m	550 m	600 m	325 m	550 m	600 m
1	3.52	2.53	2.39	15.03	16.36	16.12
2	3.52	1.98	1.82	15.03	14.25	14.02
3	3.52	1.59	1.50	15.03	13.59	13.25
4	3.52	1.47	1.09	15.03	13.23	12.91
5	5.98	1.79	1.49	14.97	14.83	14.58

3.2 Numerical Simulation from Case-6 to Case-11

Figure 5 shows the water surface profiles and velocity ones at 600m location in from Case-6 to Case-11. In Case-6, Case-7 and Case-8, the vegetation area is set on the seaside of the embankment and hollow. On the other

hand in Case-9, Case-10 and Case-11, the vegetation area is set oppositely on the landward of embankment and hollow. The effect of vegetation area in reducing the intensity of inundation flow seems small in this study because of the narrow width of the vegetation area on Lampon beach.

Due to the smaller effect of vegetation area on reducing tsunami energy, the water surface profiles and velocity ones in each figure seems similar to the results in Figure 4. Table 3 shows the maximum values of the inundated flow depth and velocity obtained from the profiles in Figure 5. In this group, Case-11 has the highest efficiency in reducing inundated flow depth and velocity. This case consists of the vegetation, embankment and hollow topography and each section is arrayed from the seaside to the landward. As discussed in previous section, this reducing function is obtained from the double flow reflection as seen in Case-4.

Table 3. Maximum inundated flow depth and velocity at 325m, 550m and 600m locations (Case-6 to Case-11)

CASE	Water height			velocity		
	325 m	550 m	600 m	325 m	550 m	600 m
6	3.52	1.49	1.40	15.03	12.46	12.27
7	3.52	1.47	1.36	15.03	12.85	12.41
8	3.52	1.91	1.55	15.03	11.92	11.85
9	3.52	1.89	1.63	15.03	12.73	12.51
10	3.52	1.58	1.34	15.03	11.70	11.37
11	3.52	1.42	1.27	15.03	11.69	11.35

Case-10 also shows good performance in reducing the inundation flow, though the efficiency seems slightly inferior to Case-11. These results mean that the embankment arranged in front of the hollow enhances the good performance in reducing the intensity of inundation flow.

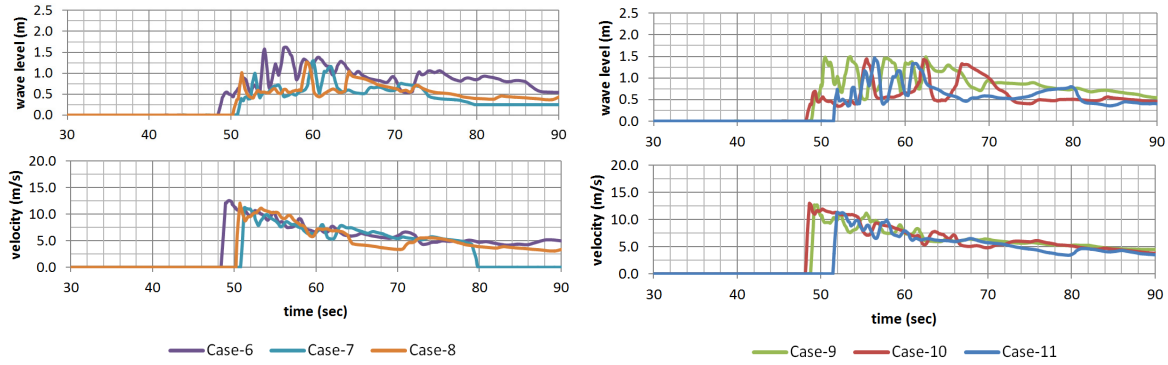

Figure 5. Profiles of inundated flow depth and velocity at 600m location (From Case-6 to Case-11)

Case-6 arranges the embankment in front of the hollow topography, and vegetation area is behind those topographies. The hydraulic performance of this case also seems slightly inferior to Case-11. Regarding the limitation of beach width, hollow and embankment topography may be arrayed after the vegetation area. This array pattern investigated in Case-9, Case-10 and Case-11 seems superior to the cases from Case-6 to Case-8.

3.3 Numerical Simulation from Case-12 to Case-16

Numerical experiments from Case-12 to Case-16 investigate the multiple-use of embankment and hollow in reducing inundated flow energy. Figure 6 shows the snapshot of tsunami inundation from Case-12 to Case-16. As shown in Case-13 and Case-15, larger flow reflection can be observed in front of the embankment which is set after hollow topography. It seems that the topography with embankment and hollow on shore side diminishes the inundated flow at first, and landward topography reduces the intensity of tsunami inundation again due to the flow reflection.

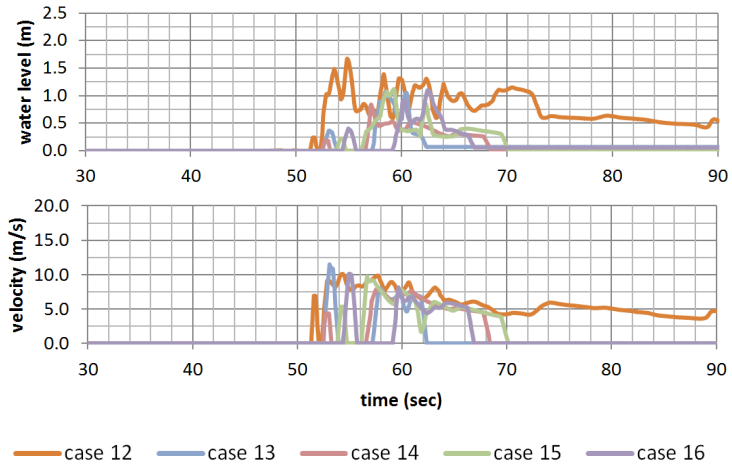

Figure 6. Profiles of inundated flow depth and velocity at 600m location (From Case-12 to Case-16)

Figure 7 shows the water surface profiles and velocity ones at 600m location from Case-12 to Case-16. It is clear that the multiple-use of hollow and embankment reduces the inundated water depth and velocity in comparison with the previous results shown in Figure 4 and Figure 5.

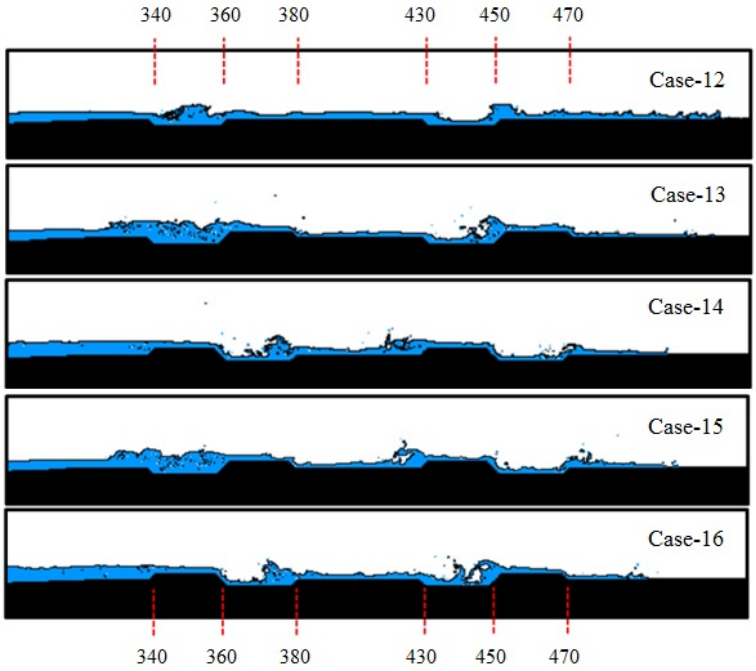

Figure 7. Snapshot of tsunami inundation at t=35 sec (Case-12 to Case-16)

Furthermore, the multiple-use of hollow and embankment extremely shortens the duration of inundation as well. This means that the mass of water inundates into landward may be reduced extremely by the multiple uses of hollow and embankment topography. Table 4 shows the maximum flow depth and velocity obtained from the profiles in Figure 6. Case-15 has the highest efficiency in reducing inundated flow depth and velocity in this group, and Case-14 and Case-16 also show similar results

Table 4. Maximum inundated flow depth and velocity at 325m, 550m and 600m locations (Case-12 to Case-16)

CASE	Water height			velocity		
	325 m	550 m	600 m	325 m	550 m	600 m
12	3.52	1.64	1.51	15.03	12.47	11.54
13	3.52	0.78	0.72	15.03	11.43	11.33
14	3.52	0.75	0.73	15.03	11.31	10.85
15	3.52	0.76	0.72	15.03	10.25	9.92
16	3.52	0.78	0.75	15.03	10.53	10.18

4. Conclusion

This study evaluates the efficiency of hollow topography, which is developed in Lampon village in Indonesia as one of the local wisdoms, in reducing tsunami inundation depth and velocity. Furthermore, this study evaluates the efficiency of other contrivances, such a parallel use of embankment and hollow topography, combination of vegetation area, and a multiple-use of hollow and embankment topography, in order to enhance the performance of countermeasures introduced as a local wisdom. This study reveals that the hollow topography has the function of reducing tsunami inundation energy. Single hollow topography reduces the velocity and water level less than 60% in comparison with the case without any measures. Furthermore, the parallel use of embankment and hollow topography could enhance the reduction of hydraulic force due to the flow reflection. The multiple-use of embankment and hollow topography extremely lower the velocity and water level, less than 15% against the case without any measures. This system also shortens the duration of inundation as well, and the system could check the mass of water inundate into landward area.

Because of the narrow vegetation area and larger porosity, effect of vegetation area on reducing tsunami inundation energy seems very small in this study. The vegetation area with enough width has the function of reducing tsunami energy, and the parallel use of vegetation area with embankment and hollow topography should be considered in future works.

Acknowledgments

This work has been supported by Department of Urban and Regional Planning, University of Brawijaya, Indonesia. The authors would like to thank the students who join this research as research assitance. We would also like to thank Directorate General of Higher Education (DGHE / DIKTI) for the financial support of this study.

References

Fukui, Y., Hidehiko, S., Nakamura, M., & Sasaki, Y. (1962). Study on Tsunami. *Annual Journal of Coastal Engineering in Japan*, *9*, 44-49. (in Japanese)

Harada, K., & Imamura, F. (2002). Experimental Study on the Effect of Reducing Tsunami by the Coastal Permeable Structures. *Proceeding of The Twelfth International Offshore and Polar Engineering Conference, ISOPE*, 652-658.

Suzuki, T., & Arikawa, T. (2010). Numerical Analysis of Bulk Coefficient in Dense Vegetation By Immersed Boundary Method. *Proceedings of the International Conference on Coastal Engineering*, *32*, 625-635.

Tsuji, Y., Imamura, F., & Matsutomi, H. (1995). Field Survey of the East Java Earthquake and Tsunami of June 3, 1994. *Pure and Applied Geophysics*, *144*(3/4), 839-854. http://dx.doi.org/10.1007/BF00874397

The Study Group for the Development of CADMAS-SURF. (2001). *CADMAS-SURF User's manual* (p. 10). (in Japanese)

Wijatmiko, I., & Murakami, K. (2010). Numerical Simulation of Tsunami Bore Pressure on Cylindrical Structure. *Annual Journal of Civil Engineering in the Ocean, JSCE*, *26*, 273-278.